

Increasing the Fisher Information Content in the Matter Power Spectrum through Lagrangian Space Reconstruction

Qiaoyin Pan,^{1,*} Ue-Li Pen,^{2,3,4,5,†} Derek Inman,^{2,6} and Hao-Ran Yu^{2,7}

¹*School of Physics, Nankai University, 94 Weijin Rd, Nankai, Tianjin, 300071, China*

²*Canadian Institute for Theoretical Astrophysics, University of Toronto,
60 St. George Street, Toronto, Ontario M5S 3H8, Canada*

³*Dunlap Institute for Astronomy and Astrophysics,
University of Toronto, Toronto, ON M5S 3H4, Canada*

⁴*Canadian Institute for Advanced Research, Program in Cosmology and Gravitation*

⁵*Perimeter Institute for Theoretical Physics, Waterloo, ON, N2L 2Y5, Canada*

⁶*Department of Physics, University of Toronto, 60 St. George, Toronto, ON M5S 1A7, Canada*

⁷*Kavli Institute for Astronomy and Astrophysics, Peking University, Beijing 100871, China*

(Dated: November 6, 2016)

A new reconstruction method using the algorithm originally aiming at improving the resolution of N-body simulation called Adaptive particle mesh (APM) is recently introduced into cosmology matter field, which is expected to give a better reconstruction from non-linear density fields to linear ones in many cases. We are motivated to adapt this method to test the information content difference, checking the effect of the reconstruction method. We reconstruct 136 non-linear density fields given by independent N-body simulations, in order to recover some of the information lost in the non-linear regime of large-scale structure. Through analyzing the power spectra of both density fields from simulations and deformation potentials from reconstructions, we find that after reconstruction, the non-linear regime of correlation matrix sinks to $k \sim 0.6$. We also find that the information content has a increase by a factor up to 30 at the translinear plateau.

PACS numbers:

I. INTRODUCTION

Power spectrum is widely used in modern cosmology to measure the matter fluctuations. In the early universe, initial Gaussian density fields can be completely described by the power spectrum, or the two-point statistics. However, gravitational instability and nonlinear large scale structure (LSS) formation drive the matter distribution highly non-Gaussian, and the galaxy distribution also follows this non-Gaussian distribution. In these cases one needs to compute higher statistics which are computationally more expensive and more difficult to interpret into initial cosmological parameters. Fisher information is usually used to quantify the amount of independent information that is contained in the power spectrum estimation.

Rimes and Hamilton [1] first studied the Fisher information as a function of scale contained in the matter power spectrum given by N -body simulations, and find that there is a plateau on trans-linear scales ($k \simeq 0.2 - 0.8 h/\text{Mpc}$), which shows that on these scales, there is a strong coupling of Fourier modes and thus the power spectrum on smaller scales, gives little additional independent information. [Apart from numerical trend, Fisher information was also estimated in data from observation. For example, Lee and Pen \[2\] measured the information content in the galaxy angular power spectrum with the help of the Rimes-hamilton technique, and also found that the information saturation.](#)

There are many approaches to recover the lost information in the power spectrum of matter density field, by reversing the final density field into a more Gaussian, early stage density field. For example, Gaussianization transforms are commonly used [3, 4] to make the logarithmic distribution more Gaussian. Nonlinear Wiener filters are used in wavelet space to Gaussianize the fields and can also improve the Fisher information [5–7]. It is shown in [7] that, although these methods or their combinations may have different abilities to recover the Fisher information, by means of reducing the mode coupling and variances in the auto power spectrum of Gaussianized density fields, they do not necessarily improve the cross correlation (propagator in their context) between the initial density field and the final density field, and thus result in a smearing out of the baryonic acoustic oscillations (BAO) peak in the two-point correlation function. If one concerns about mapping the initial conditions to final conditions (e.g. measurement of BAO) these methods are unable to extract valid information from initial conditions, at least in the cross power spectrum between initial and final conditions.

Reconstruction techniques (including the one described in [7]) are able to increase the Fisher information while also improve the cross correlation to the initial conditions and sharpen the BAO peak. It is based on the coupling of linear density field $\delta_L(\mathbf{q}, t_0)$ to the displacement field $\Psi(\mathbf{q})$, first derived by [8], and the displacement field is estimated by a smoothed final density field. [9] show a new method in the estimation of displacement field in 1-dimensional (1D), according to which the 1D linear density field is reconstructed in Lagrangian space and successfully improve the BAO measurement. In 3D cases, it is nontrivial to estimate the displacement field,

*Electronic address: panda@mail.nankai.edu.cn

†Electronic address: pen@cita.utoronto.ca

but [10] show that the displacement field given by N -body simulations can be used to recover the δ_L .

In this paper we generalize the displacement field estimation method from 1D [9] to 3D, and reconstruct δ_L and study the Fisher information recovery in δ_L . Here, the displacement field estimation is done by a moving-mesh (MM) algorithm, which is based on the adaptive particle-mesh (APM) simulation algorithm [11, 12].

Neyrinck, Szapudi and Rimes [13] argued that more information could be extracted on non-linear scales if the masses of the largest haloes in a survey are known. Neyrinck, Szapudi and Szalay [4] found that nonlinearities in the dark-matter power spectrum are dramatically smaller if the density field first undergoes a logarithmic mapping, yielding 10 times more cumulative signal-to-noise at $z = 0$. Zhang et al. [5] suggested that using Wavelet Wiener filter to separate Gaussian and non-Gaussian structure in wavelet space is possible to increase the Fisher information by a factor of three before reaching the translinear plateau. Similar steps was also done in the angular power spectrum of weak lensing [6] and the result showed that there's three times more information compared to that of logarithmic mapping. Later, Neyrinck [14] applied Gaussianizing transformation method to cosmology and found that it can greatly multiply the Fisher information. Simpson, Heavens and Heymans utilized Clipping [15] technique on the matter density field and found it increased the number of useful Fourier modes by more than two orders of magnitude.

Pen [11, 12] introduced new N-body algorithm call Adapted Particle-mesh (APM), which scaled linearly with the number of particles for the computational effort per time step, aiming at offering higher resolution. This method can be used to reconstruct the matter density field and is hopeful for tracing a non-linear density field back to it's linear part[9].

This paper is organized as follows. In Section II, we present the main steps of the N -body simulation code that was used to simulate the dark matter density fields. In Section III, we briefly describe the reconstruction algorithm. In Section IV, we calculate and compare the power spectra, correlation matrix and Fisher information given by simulation and reconstruction. Conclusion and discussion are presented in Section V

II. N-BODY SIMULATION OF DARK MATTER DENSITY FIELDS

We run 136 simulations with a box size of $300 h^{-1} \text{Mpc}$, resolution of 1024^3 cells and 512^3 particles, using the cosmological simulation code CubeP3M[16]. The initial condition is given by reading the transfer function computed by CAMB[17] and then evolving the power linearly to $z = 100$. Then Zel'dovich approximation is used to calculate the displacement field and velocity field, which are assigned to the particles. The cosmological parameters used are $\Omega_M = 0.32$, $\Omega_\Lambda = 0.679$, $h = 0.67$, $\sigma_8 = 0.83$, and $n_s = 0.96$. And we use different seeds to produce the initial conditions for different simulations so that those

simulations are independent to each other. Then the initial densities are evolved up to $z = 0$.

III. RECONSTRUCTION ALGORITHM

We use the algorithm and numerical method called Adaptive Particle-mesh (APM), discribed in [11, 12]. to reconstruct the density field. The basic idea is to build a PM scheme on a curvilinear coordinate system, in which the number of the particles per grid cell is set approximately constant. Consider a numerical grid of curvilinear coordinates $\xi = (\xi_1, \xi_2, \xi_3)$. In order to determine the physical position of each grid point, one needs to specify the Euclidean coordinate $\mathbf{x}(\xi, t)$ as a function of grid position. In the Euclidean coordinate, the flat metric is Kronecker delta function δ_{ij} , while the curvilinear metric is given by

$$g_{\mu\nu} = \frac{\partial x^i}{\partial \xi^\mu} \frac{\partial x^j}{\partial \xi^\nu} \delta_{ij}. \quad (1)$$

We use the convention that Latin indices denote Cartesian coordinate, while Greek indices denote the curvilinear grid coordinate. In principle, there are many different methods to connect the Cartesian coordiante and curvilinear coordinate of each grid cell. In APM method, the connetction is described by an irrotational deformation,

$$x^i = \xi^\mu \delta_\mu^i + \Delta x^i, \quad (2)$$

where

$$\Delta x^i = \frac{\partial \phi}{\partial \xi^\nu} \delta_\nu^i. \quad (3)$$

This choice of the deformation can minimize mesh distortion and twisting. ϕ is called the deformation potential, and Δx^i the lattice displacement. The deformation potential can be given in terms of the continuity equation in curvilinear coordinate,

$$\frac{\partial \sqrt{g} \rho}{\partial t} + \partial_\mu [\rho \sqrt{g} e_\mu^i (v^i - \Delta x^i)] = 0 \quad (4)$$

where $\sqrt{g} \equiv (\partial x^i / \partial \xi^\alpha)$ is the volume element and $e_\mu^i = \partial \xi^\mu / \partial x^i$ is the triad. $\Delta x = \delta^{i\nu} \partial_\nu \phi$ is chosen such that the first term in equation 4 is zero, resulting in a constant mass per volume element. And the velocity field divergence is replaced by the deviation density field $\Delta \rho = \bar{\rho} - \rho \sqrt{g}$, which ideally should be zero. Then the deformation potential is described in the elliptic equation,

$$\partial_\mu (\rho \sqrt{g} e_\mu^i \delta^{i\nu} \partial_\nu \Delta \phi) = \Delta \rho \quad (5)$$

The equation 5 can be solved using multigrid algorithm described in Ref. Then the displacement is given by the gradient of the deformation potential as in 3. One layer of the deformed grids and the original density field of that layer is given in Fig. II. As expeted, there's no grid crossing after reconstruction.

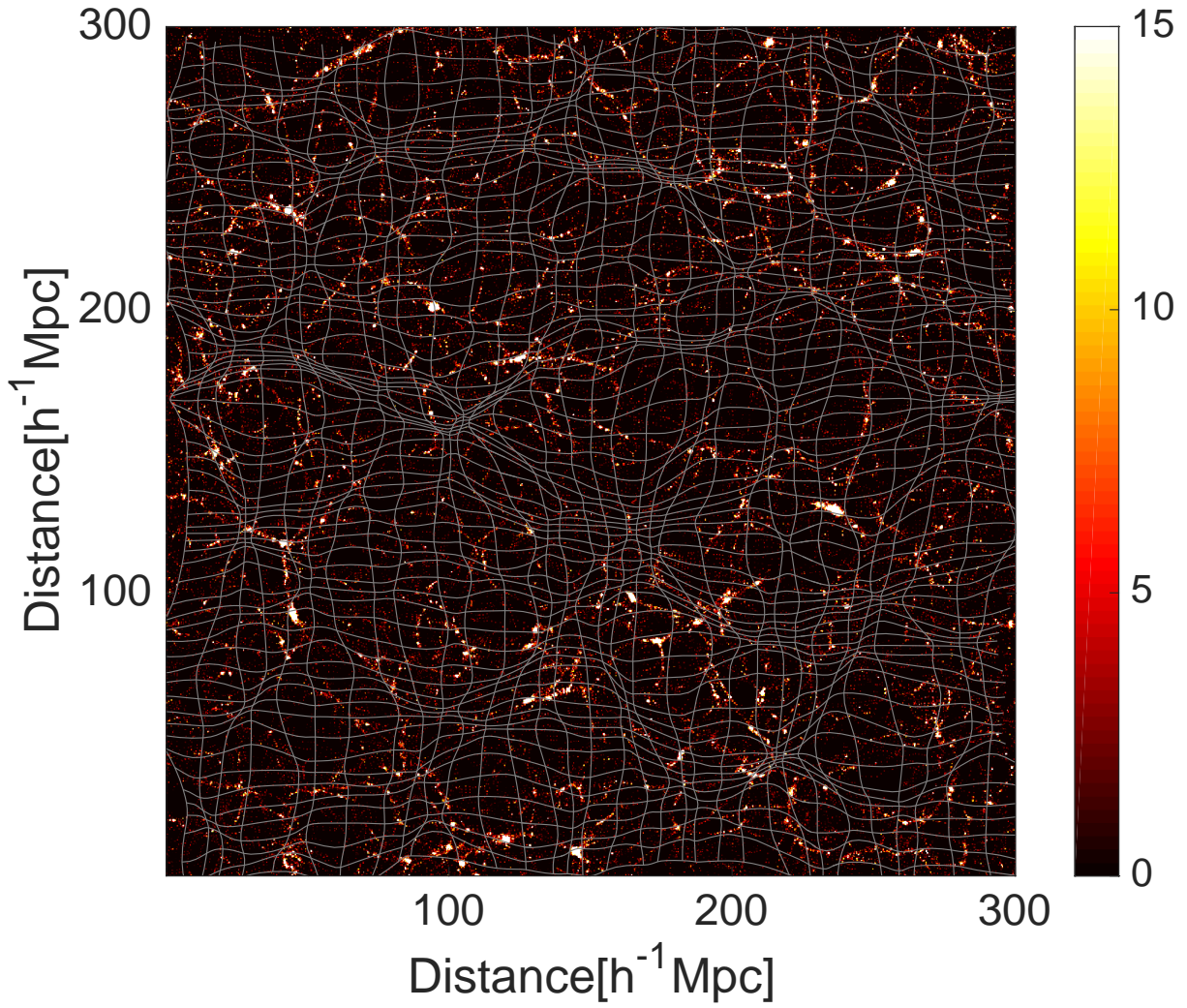


FIG. 1: Map of a randomly selected layer of a randomly selected density field from 136 N-body simulations, with a $300 h^{-1}\text{Mpc}$ width box and 1024^3 pixels. The magnitude is the average of number of particles per cell. And the deformed grids of the selected density field.

IV. POWER SPECTRA AND INFORMATION CONTENT

The power spectrum is the Fourier transform of the correlation function and measures the amount of clustering in the matter distribution in terms of the wavenumber k in unit of $h\text{Mpc}^{-1}$,

$$\langle \delta(\mathbf{k}) \delta(\mathbf{k}') \rangle = (2\pi)^3 P(\mathbf{k}) \hat{\delta}(\mathbf{k} - \mathbf{k}'), \quad (6)$$

where $\delta(\mathbf{k})$ is the density fluctuation in wave space, while $\hat{\delta}$ is the delta function. Of equal interest is Δ_k^2 , the power spectrum in its dimensionless form, defined as

$$\Delta_k^2 \equiv \frac{k^3 P(k)}{2\pi^2} \quad (7)$$

The power spectra of the mass distributions are calculated using the "Nearest Grid Point" (NGP) mass assignment scheme, which calculates the position of each particle based on which grid point it is nearest. In Fig.??

we plot the mean power spectrum (and error bars) of 136 linear and non-linear density fields and reconstructed density fields simply given by $\delta_r = \mathbf{k}\mathbf{k}\xi$. The linear density field is given by the linear density field at $z = 0$. To calculate the cumulative Fisher information of the density fields, the covariance matrix of the power spectra should be first given. Mathematically, the covariance matrix is defined as

$$\text{Cov}(k, k') \equiv \frac{1}{N-1} \sum_{i=1}^N [P_i(k) - \langle P(k) \rangle] [P_i(k') - \langle P(k') \rangle], \quad (8)$$

where angle brackets mean the expected values. The cross-correlation coefficient matrix, or for short, the correlation matrix, is a normalized version of the covariance matrix,

$$\text{Corr}(k, k') = \frac{\text{Cov}(k, k')}{\sqrt{\text{Cov}(k, k) \text{Cov}(k', k')}}. \quad (9)$$

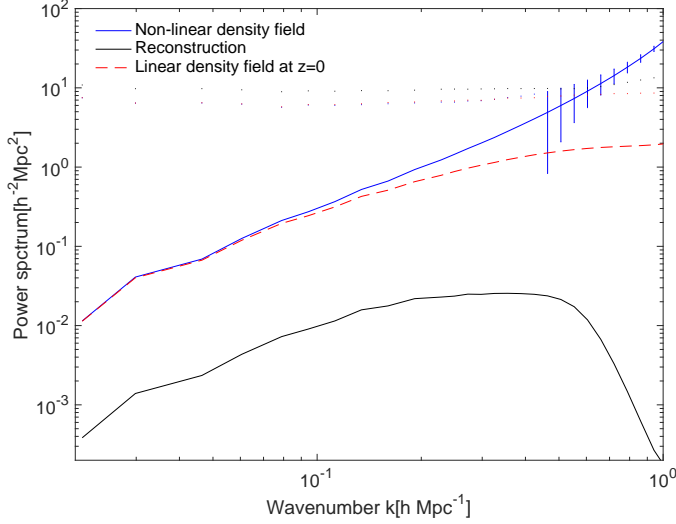


FIG. 2: Mean power spectrum with error bar of 136 linear density fields, non-linear density fields and reconstructed density fields.

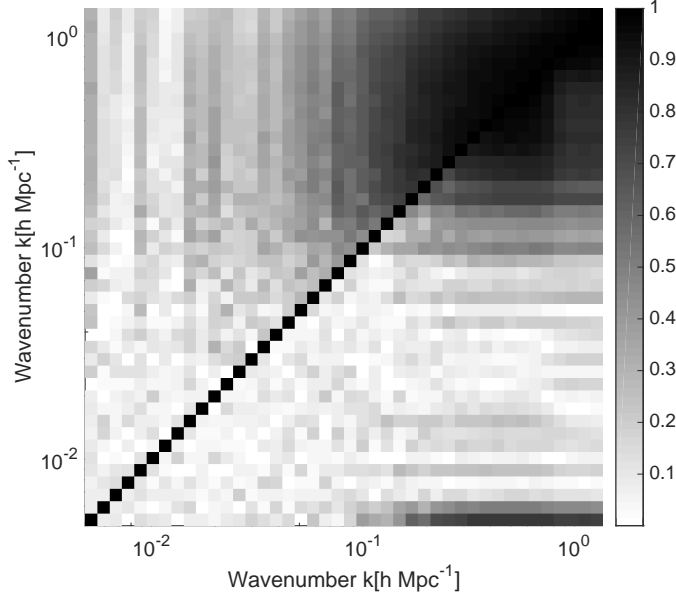


FIG. 3: Cross-correlation coefficient matrix as found from 136 power spectra of the non-linear density field from simulation (the upper triangle) and the deformation potential field from reconstruction (the lower triangle).

The correlation matrices for density fields from simulations and deformation potentials from reconstructions are shown in Fig. 3. For the original density fields, the linear regime, where $k < 0.1$, is diagonal, while in the non-linear regime, the power spectra of different k modes are strongly correlated by at least 60%. For the reconstructed deformation potential correlation matrix, however, the linear regime expand up to k 0.2. The correlation matrix is closer to that for the power spectra of linear density fields. The cumulative, or Fisher, information function of k_n is then defined as the sum of the elements of inverse of subsection of the normalized

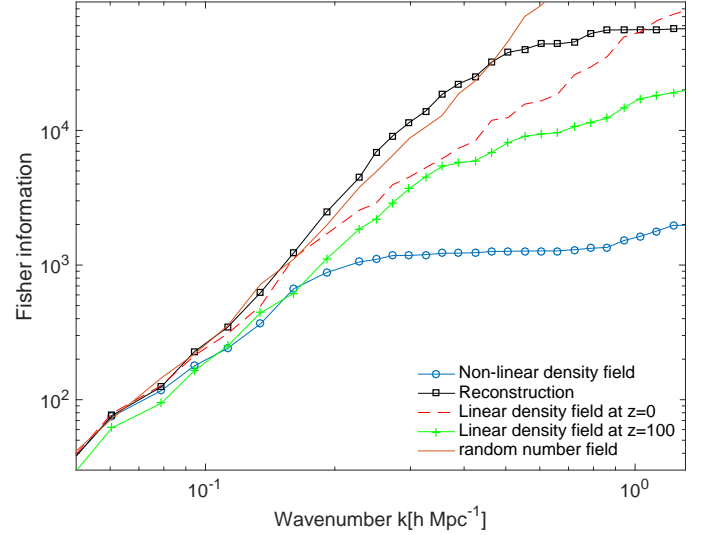


FIG. 4: Cumulative information in the power spectra as a function of wavenumber. The blue cycles correspond to the non-linear density field by simulation; the black squares correspond to the the reconstructed deformation potential; the red dash line corresponds to linear density field at $z = 0$; the green crosses correspond to linear density field at $z = 100$.

covariance matrix up to k_n scale

$$I(< k_n) = \sum_{i,j=1}^n [C_{norm}^{-1}(k_i, k_j)] (i, j \leq n), \quad (10)$$

where C_{norm} is the normalized covariance matrix, defined as

$$C_{norm}(k, k') = \frac{\text{Cov}(k, k')}{\langle P(k) \rangle \langle P(k') \rangle}. \quad (11)$$

As seen above, cumulative information is a measurement of the number of independent Fourier modes presented in a field up to a given k_n , which represents how linear a field is. We plot the cumulative information of the power spectra of density fields from simulations and deformation potentials from reconstructions in Fig. 4. In the translinear regime, where $k \sim 0.1$, the cumulative information of the non-linear density field has a flat plateau. It indicates that there's nearly no independent information in the translinear regime of the power spectrum. At $k \sim 0.8$, the information increase slightly again. But the information curve of the reconstructed deformation potential keeps increasing and reaches its plateau at $k \sim 0.6 - 0.7$ up to a factor of 20. It indicates that APM method can strongly recover the lost information within this scale.

V. CONCLUSION AND DISCUSSION

We use the code "CubeP3M" to generate 137 independent dark matter density fields, then give the reconstructed deformation potentials which are pure divergent

using APM method. We analyze the power spectra of both the density fields and the deformation potentials, after which we give the cross correlation matrix. We find that the power spectra are highly correlated on small scales, since these scales are in non-linear regime. But after reconstruction, the strongly correlated regime sinks from $k \sim 0.1$ to $k \sim 0.6$. We also calculate the cumulative information, and find that the plateau of the reconstructed information curve in the tranlinear regime rises by a factor of 30.

The new reconstruction method successfully recovers the lost linear information on the mildly non-linear scale, at least twice better than previous methods [4–6, 13, 14] and pushes the non-linear scale to a smaller scale in our case. The result in dark matter density fields gives a strong motivation to adapt APM method in halo fields, neutrino fields, etc, so that we have access to know more clearly about the physics in smaller scale. Some efforts were made to improve cosmology measurements to BAO scale (e.g. [18, 19]). APM gives the reconstructed displacement given on the Lagrangian coordinate instead of the final Eulerian coordinate. It's successful try of BAO

reconstruction in 1-D cosmology [9] provided an intuitive view of the algorithm to develop the BAO reconstruction in 3-D and thus push forward the BAO research.

APM method effectively decomposes the irrotational part and the curl part of the displacement field of particles, which would be meaningful to be compared with the decomposition of displacement field given by N-body simulation [10].

Acknowledgments

We thank Hong-Ming Zhu and Xin Wang for friendly and helpful discussions. Computations were performed on the General Purpose Cluster supercomputer at the SciNet HPC Consortium. SciNet is funded by: the Canadian Foundation for Innovation under the auspices of Compute Canada; the Government of Ontario; Ontario Research Fund - Research Excellence; and the University of Toronto.

-
- [1] C. D. Rimes and A. J. S. Hamilton, in *American Astronomical Society Meeting Abstracts #207* (2006), vol. 207 of *American Astronomical Society Meeting Abstracts*, p. 206.01.
 - [2] J. Lee and U.-L. Pen, *ApJ* **686**, L1 (2008), 0807.1538.
 - [3] D. H. Weinberg, *MNRAS* **254**, 315 (1992).
 - [4] M. C. Neyrinck, I. Szapudi, and A. S. Szalay, *ApJ* **698**, L90 (2009), 0903.4693.
 - [5] T.-J. Zhang, H.-R. Yu, J. Harnois-Déraps, I. MacDonald, and U.-L. Pen, *ApJ* **728**, 35 (2011), 1008.3506.
 - [6] H.-R. Yu, J. Harnois-Déraps, T.-J. Zhang, and U.-L. Pen, *MNRAS* **421**, 832 (2012), 1012.0444.
 - [7] J. Harnois-Déraps, H.-R. Yu, T.-J. Zhang, and U.-L. Pen, *MNRAS* **436**, 759 (2013), 1205.4989.
 - [8] Y. B. Zel'dovich, *A&A* **5**, 84 (1970).
 - [9] H.-M. Zhu, U.-L. Pen, and X. Chen, *ArXiv e-prints* (2016), 1609.07041.
 - [10] H.-R. Yu, U.-L. Pen, and H.-M. Zhu, *ArXiv e-prints* (2016), 1610.07112.
 - [11] U.-L. Pen, *ApJS* **100**, 269 (1995).
 - [12] U.-L. Pen, *ApJS* **115**, 19 (1998), astro-ph/9704258.
 - [13] M. C. Neyrinck, I. Szapudi, and C. D. Rimes, *MNRAS* **370**, L66 (2006), astro-ph/0604282.
 - [14] M. C. Neyrinck, in *Statistical Challenges in 21st Century Cosmology*, edited by A. Heavens, J.-L. Starck, and A. Krone-Martins (2014), vol. 306 of *IAU Symposium*, pp. 251–254, 1407.4815.
 - [15] F. Simpson, A. F. Heavens, and C. Heymans, *Phys. Rev. D* **88**, 083510 (2013), 1306.6349.
 - [16] J. Harnois-Déraps, U.-L. Pen, I. T. Iliev, H. Merz, J. D. Emberson, and V. Desjacques, *MNRAS* **436**, 540 (2013), 1208.5098.
 - [17] A. Lewis, A. Challinor, and A. Lasenby, *ApJ* **538**, 473 (2000), astro-ph/9911177.
 - [18] D. J. Eisenstein, H.-J. Seo, E. Sirko, and D. N. Spergel, *ApJ* **664**, 675 (2007), astro-ph/0604362.
 - [19] M. White, *MNRAS* **450**, 3822 (2015), 1504.03677.
-